Flow-based arterial spin labeling: from brain to body

Franklin, S.L.

Chapter 3

Multi-organ comparison of flow-based arterial spin labeling techniques: Spatially non-selective labeling for cerebral and renal perfusion imaging.

S.L. Franklin[1,2,3], I.K. Bones[2], A.A. Harteveld[2], L. Hirschler[1], M. van Stralen[2], Q. Qin[4], A. de Boer[2], H. Hoogduin[2], C. Bos[2], M.J.P. van Osch[1,3], S. Schmid[1,3].

[1]C.J. Gorter Center for High Field MRI, Department of Radiology, Leiden University Medical Center, Leiden, The Netherlands
[2]Center for Image Sciences, University Medical Center Utrecht, Utrecht, The Netherlands
[3]Leiden Institute for Brain and Cognition, Leiden University, Leiden, The Netherlands
[4]The Russell H. Morgan Department of Radiology and Radiological Science, Division of MR Research, Johns Hopkins University School of Medicine, Baltimore, Maryland, USA.

Published as full paper in: Magnetic Resonance in Medicine, 2021; 85(5): 2580-2594.

ABSTRACT

Purpose: Flow-based arterial spin labeling (ASL)-techniques provide a transit-time insensitive alternative to the more conventional spatially-selective ASL-techniques. However it is not clear which flow-based ASL-technique performs best, and also, how these techniques perform outside the brain (taking into account e.g. flow-dynamics, field-inhomogeneity, organ motion). In the current study we aimed to compare four flow-based ASL-techniques (i.e. velocity selective ASL, acceleration selective ASL, multiple velocity selective saturation ASL, and velocity selective inversion prepared ASL (VSI-ASL)) to the current spatially-selective reference techniques in brain (i.e. pseudo-continuous ASL (pCASL)) and kidney (i.e. pCASL and flow alternating inversion recovery (FAIR)).

Methods: Brain (n=5) and kidney (n=6) scans were performed in healthy subjects at 3T. Perfusion-weighted signal (PWS-) maps were generated and ASL-techniques were compared based on temporal signal-to-noise-ratio (tSNR), sensitivity to perfusion changes using a visual stimulus (brain) and robustness to respiratory motion by comparing scans acquired in paced-breathing and free-breathing (kidney).

Results: In brain, all flow-based ASL-techniques showed similar tSNR as pCASL, but only VSI-ASL showed similar sensitivity to perfusion changes. In kidney, all flow-based ASL-techniques had comparable tSNR, though all lower than FAIR. In addition, VSI-ASL showed a sensitivity to B_1-inhomogeneity. All ASL-techniques were relatively robust to respiratory motion.

Conclusion: In both brain and kidney, flow-based ASL-techniques provide a planning-free and transit-time insensitive alternative to spatially-selective ASL-techniques. VSI-ASL shows the most potential overall, showing similar performance as the golden standard pCASL in brain. However, in kidney a reduction of B_1-sensitivity of VSI-ASL is necessary to match the performance of FAIR.

INTRODUCTION

Arterial spin labeling (ASL) is a non-invasive technique which can be applied in various organs to measure tissue perfusion. Traditionally, ASL employs spatially-selective labeling of the blood to generate an endogenous tracer. In spatially-selective labeling techniques, label is created proximal to the region of interest (ROI), after which a delay is inserted to allow the labeled blood to travel from the labeling location to the ROI. The currently recommended spatially-selective ASL-technique in the brain is pseudo-continuous ASL (pCASL) [13].

However, quantification issues can arise due to the time it takes for the labeled blood to flow from the labeling location to the ROI, i.e. transit-time. For a subject with slow blood flow, transit-times can become so long that the label-signal has decayed before it reaches the ROI. Setting the transit-times to match the delay times would lead to severe signal-to-noise-ratio (SNR)-loss. While setting the delay times too short would lead to label still residing in the vascular compartment, making it impossible to discriminate between tissue that would be perfused later or tissue that would not be perfused at all, something which is often crucial for diagnosis or treatment selection.

Recently, a number of flow-based ASL-techniques have been introduced where blood is labeled based on its flow velocity or acceleration instead of spatial location. Flow-based ASL-techniques create label also within the ROI, making them less sensitive to transit-delays[43], [95]–[97]. Reduced sensitivity to transit-delays is especially valuable in cases where blood flow is slow, e.g. in elderly[98], patients with MoyaMoya disease[43], [95], [99] or in patients with renal artery stenosis[100], [101].

Moreover, flow-based ASL-techniques do not require planning of a spatial labeling volume, making it easier and more time-efficient to apply in practice. Planning of a spatial labeling volume can be especially challenging in the abdomen due to respiratory motion and (dynamic) field-inhomogeneities[13], [102], [103]. In the kidneys for example, ASL has been recognized as a promising tool to assess kidney function and identify pathology non-invasively[18], [100], [104], but planning of the labeling slab for renal ASL can be time-consuming and requirements for placement of the labeling slab can restrict the part of the kidney that is imaged[62]. Flow-based ASL can overcome these challenges, making it an interesting alternative to measure renal perfusion.

The first flow-based ASL-technique, which is partly based on early suggestions by Norris and Schwarzbauer[105], was proposed by Wong et al. (2006)[49]: velocity-selective ASL (VSASL) uses motion-sensitized gradients (MSGs) to saturate blood magnetization above a certain cut-off velocity in the label condition, generating ASL-signal based on the blood flow velocity.

VSASL was followed by acceleration-selective ASL (AccASL)[51], where signal is created based on differences in blood flow acceleration(deceleration) instead of velocity. In 2015, multiple velocity-selective ASL (mm-VSASL)[52] was proposed, in which additional velocity selective saturation (VSS)-labeling modules are used, to increase the amount of label created and thus increase SNR. Lastly, velocity-selective inversion prepared ASL (VSI-ASL) was proposed. VSI-ASL uses a Fourier-transform based velocity-selective pulse train to generate label based on inversion of magnetization[53], potentially doubling SNR compared to the saturation-based techniques. Whereas all of these techniques have their individual advantages and challenges, it is still unclear which technique is the most effective for perfusion measurements.

The aim of this study was to perform a direct comparison of these four flow-based techniques to the currently recommended spatially-selective labeling techniques. This comparison was made both for brain as well as for kidney applications since the use of ASL is no longer restricted to just the brain. Moreover, flow-based ASL is hypothesized to behave differently in brain and kidney, because of differences in flow-dynamics, B_0/B_1 field homogeneity, and organ motion.

In brain, flow-based ASL-techniques were compared to pCASL, the golden standard in brain, based on temporal SNR (tSNR). In addition, sensitivity to identify perfusion changes was investigated using a visual task. In kidney, the flow-based techniques were compared to the recommended methods in kidney; pCASL and FAIR[62], based on tSNR. In addition, robustness to respiratory motion was investigated by performing all scans both in paced- and free-breathing. Moreover, this is to the best of our knowledge, the first time that AccASL, mm-VSASL, and VSI-ASL are applied in kidney.

THEORY

Figure 1 shows the sequence diagrams for all flow-based ASL-techniques used in the current study. The VSASL-sequence uses VSS-labeling and control modules. VSS-modules consist of two adiabatic hyperbolic secant inversion pulses and two 90-degree hard pulses[49]. Labeling is based on MSGs. The MSGs are only present in the label-module, so that under the assumption of a laminar flow profile, the magnetization of spins flowing above a cut-off velocity is saturated[49]. The last VSS-module in the sequence, right before the image acquisition, has MSGs in both label and control-condition. It acts as a crusher for the labeled blood that has moved into the venous compartment and is accelerating, and labeled blood that is still flowing above the cut-off velocity in the large vessels; moreover, it results in a predefined temporal width of the bolus of labeled spins as required for blood flow quantification. Mm-VSASL uses the same VSS-modules, but has an additional label VSS-module (Figure 1d).

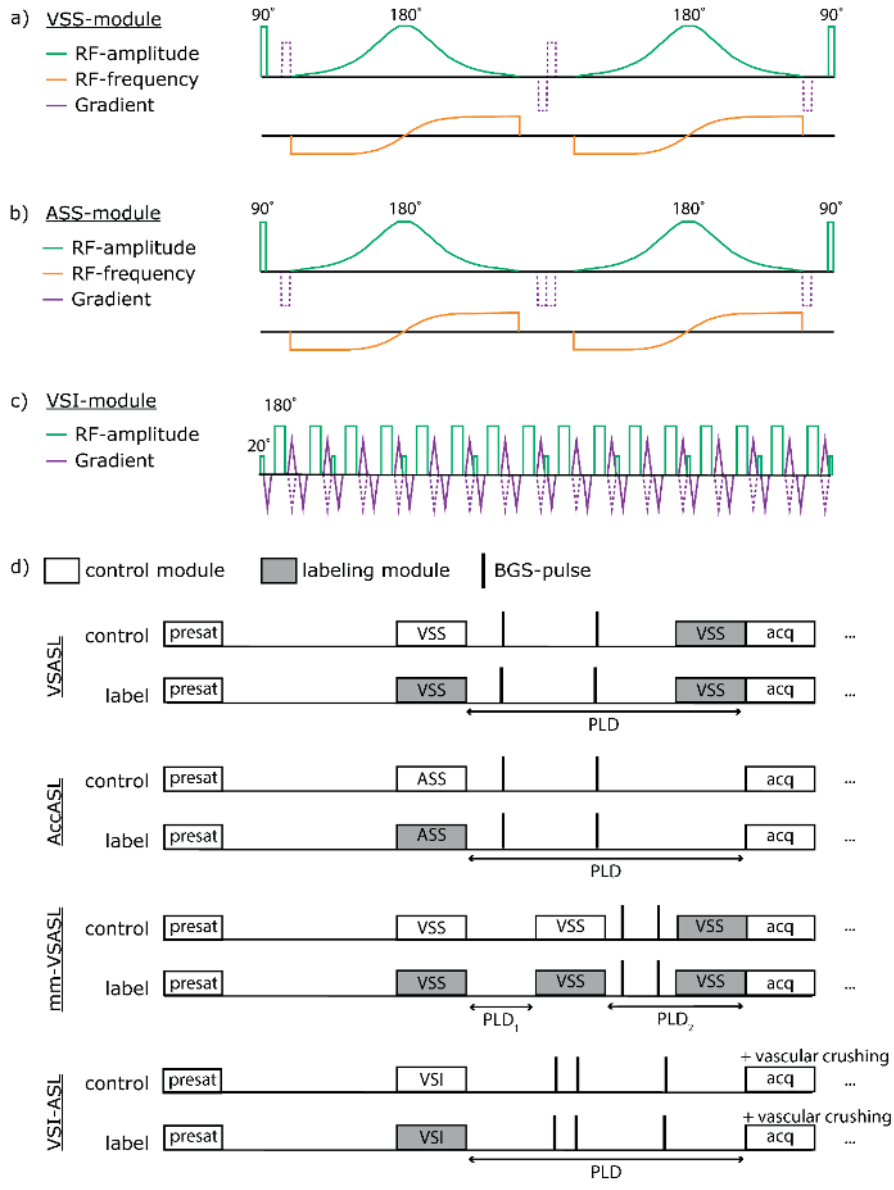

Figure 1. A) A velocity selective saturation (VSS) label/control module is shown, including two 90-degree hard RF-pulses, two adiabatic hyperbolic secant RF-pulses, and motion-sensitized gradients (MSG) in the label condition, as described in Wong et al.[49]. *These VSS-modules are also used for mm-VSASL* [52]. *In B) an acceleration selective saturation (ASS) label/control module is shown, it consists of the same RF-pulses as in the VSS-module, only here the polarity of the MSG is only negative instead of alternating, as described in Schmid et al.* [51]. *Also for AccASL the MSG are only added in the label module. In C) a velocity selective inversion (VSI) label/control module is shown including nine 20-degree hard RF-pulses and sixteen phase-cycled 180-degree hard RF-pulses and eight sets of MSGs, as described in Qin and van Zijl*[53]. *In the label module the gradients have alternating polarity, while in the control module the polarity is solely negative. In D) Schematic sequence diagrams of the flow-based ASL-sequences; VSASL, AccASL, mm-VSASL, and VSI-ASL, incorporating the VSS, ASS and VSI-modules shown in a-c. Gray block represent the label modules, white blocks the control modules and the thick stripes represent the background suppression (BGS-) pulses. A WET module*[84], [107] *is used as presaturation (presat) and multi-slice single-shot GE-EPI is used for acquiring images (acq). Image is not drawn to scale.*

AccASL uses acceleration-selective saturation (ASS-) modules. The MSGs in the ASS-modules are similar to ones in VSS-modules, albeit played out with a negative polarity, leading to a phase-dependence on spin acceleration(deceleration) instead of velocity (Figure 1b)[51]. By subtracting label from control signal, signal is generated only from the spins with an acceleration (or deceleration) above the cut-off[51], [106]. AccASL has not been implemented yet using a second labeling module[51]. This makes quantification of the AccASL-signal currently not possible, since the temporal width of the bolus would be unknown.

VSI-ASL is based on a slightly different principle. VSI-modules incorporate a Fourier-transform based velocity-selective pulse train in the form of nine 20-degree hard pulses in combination with sixteen phase-cycled 180-degree hard pulses to achieve inversion of the magnetization in small steps, see Figure 1c. Labeling of spins above the cut-off velocity is achieved by employing bipolar MSGs in the label-condition and negative polarity gradients in the velocity-compensated control-condition, see Figure 1d[53]. This leads to an inverted magnetization for spins flowing below the cut-off velocity during the label condition and an inverted magnetization of all spins during the control-condition[53]. In VSASL and mm-VSASL, a VSS-module right before image acquisition is used to crush the venous and vascular contribution to the ASL-signal and to enable quantification. In VSI-ASL, vascular crushing was enabled for the same purpose. Here the crushing of spins above the cut-off velocity is performed during the acquisition instead of right before. No major differences between the two approaches were found previously[49].

METHODS

Data acquisition

All flow-based ASL-techniques (VSASL, AccASL, mm-VSASL, VSI-ASL) were acquired in the brain and kidneys, and compared to the reference ASL-technique(s) in the respective anatomies.

Data was acquired on 3T Philips scanners and this study was performed with approval of the local institutional review board. Written informed consent was obtained from each subject before inclusion. Brain and kidney scans were acquired in separate scan sessions and separate subjects.

Brain

For brain, pCASL is currently the standardized ASL-technique[13], and was thus used as reference-technique. The brain scan sessions consisted of two conditions; all ASL-techniques were first acquired while the subject was watching a cartoon and a second time with eyes

closed. Within each condition the order of the ASL-techniques was randomized. The visual stimulus is expected to induce a perfusion increase in the visual cortex. By subtracting the perfusion signal during rest and visual stimulus, the sensitivity to detect small increases in perfusion can be measured for each ASL-technique.

Five healthy subjects (24-60 years, 2 male and 3 female) were included. Images were acquired using a 32ch-head coil and a multi-slice single-shot gradient-echo EPI acquisition. Image acquisition was planned in oblique transversal orientation, parallel to the corpus callosum in sagittal view. Scan parameters for VSASL, AccASL, mm-VSASL and VSI-ASL were chosen based on previous research[49], [51]–[53], see Table 1. The PLDs of flow-based ASL-techniques are usually shorter than those of spatially-selective techniques, since labeling takes place in or close to the microvascular bed. The PLD of flow-based ASL can, however, not be chosen too small, since the PLD also controls the bolus duration: only spins that have decelerated below the cut-off velocity during the PLD will contribute to the perfusion signal. mm-VSASL thus requires a slightly longer total PLD to also allow the spins saturated by the second module to decelerate. For the current study the PLD-settings were taken from the quoted literature.

The duration of the VSASL-, AccASL-, and mm-VSASL labeling modules were set to 50ms, to allow enough time for an adiabatic angle of 1500 degrees for the hyperbolic secant refocusing pulses. Gradient orientation for VSASL, AccASL and mm-VSASL was in the slice-direction i.e. feet-head direction. The number of repetitions was kept constant between all ASL-scans. Background suppression (BGS) using hyperbolic secant pulses was applied in all sequences, resulting in 85-90% suppression of tissue signal for the first slice. All ASL-techniques except for VSI-ASL employed two BGS-pulses. VSI-ASL employed three BGS-pulses to compensate the static-tissue inversion performed by the VSI-ASL modules. This makes sure that the static tissue signal is positive upon image acquisition. The exact BGS-pulse timings are reported in Table 1; defined from the end of the VSS-labeling module, and in case of mm-VSASL the end of the second VSS-labeling module. WET-presaturation[84], [107] was used to avoid spin history effects (Figure 1d), and the TR was adjusted to accommodate a 2s recovery of the WET-presaturation for all flow-based ASL-techniques. In case of pCASL, the WET-presaturation was placed right before labeling and thus did not require a TR-adjustment to accommodate regrowth of the magnetization.

A sagittal and coronal phase-contrast enhanced MRA localizer was used to aid planning of the pCASL labeling slab, using an encoding velocity of 40cm/s and a total scan duration of 54s. The pCASL labeling slab was planned perpendicular on the dorsal part of the vertebral arteries at the height of C1/C2.

An M_0-scan, for calibration of the ASL-signal, was acquired using the same acquisition as the ASL-scans with ASL-labeling turned off and using a TR of 10s. A 3D-T_1w scan, for gray matter segmentation, was acquired using a multi-shot 3D-TFE acquisition, with a TR/TE of 9.7/4.6ms, acquisition voxel size of 1.2/1.2/1.2mm, resulting in a total scan duration of 5min.

Kidney

For kidney, both pCASL and FAIR are recommended[62], and thus both were used as reference-techniques. The kidney scan sessions consisted of two conditions; all ASL-techniques were first acquired in paced-breathing, and a second time in free-breathing. Within each condition the order of the ASL-techniques was randomized. In the paced-breathing condition subjects were asked to synchronize their breathing with the image acquisition, i.e. to perform a shallow breath in and out in between the acquisitions and to hold their breath briefly on exhalation during the acquisition. The researcher provided coaching for the first couple of breaths via the intercom. Subject cooperation was checked using a respiratory bellow for both breathing conditions. Robustness to breathing strategy was investigated by comparing the tSNR per unit time during paced- and free-breathing.

Six healthy subjects (23-30 years, 3 male and 3 female) were included. Images were acquired using a 28-element phased-array body coil and a multi-slice single-shot gradient-echo EPI acquisition. Image acquisition was planned in coronal-oblique orientation, parallel to the muscles anterior to the kidney, to minimize through-slice motion. Optimal scan parameters for renal imaging were not known for all flow-based ASL-techniques, so they were chosen partly based on previous research[36], [97], [108] and partly on preliminary experiments (Table 1). The durations of the VSS- and ASS-labeling modules were set to 50ms, and gradient orientation to the slice-direction, i.e. anterior-posterior direction, to minimize effects of respiratory motion on labeling[97]. FAIR was implemented as described in[108], including Q2TIPS[109] which was placed anterior to the imaging acquisition with a 10mm gap (Table 1).

For all ASL-scans the number of repetitions was kept constant. BGS using hyperbolic secant pulses was applied in all sequences, resulting in 85-90% suppression of tissue signal for the first slice. WET-presaturation[84], [107] was used to avoid spin history effects (Figure 1d) and saturation slabs were placed superior and inferior to the imaging volume to minimize fold-in artefacts. RF-shimming was performed on a volume shim box that covered the image acquisition volume with an additional 10mm on each side in the AP-direction. B_0-shim was set to automatic. A TR of 6500ms was used for the paced-breathing scans to keep the breathing-rhythm as natural as possible. For the free-breathing scans the TR was adjusted to accommodate a 3s recovery of the saturation slabs and WET-presaturation.

Scan parameter	**VSASL**[49]	**AccASL**[51]	**mm-VSASL**[52]	**VSI-ASL**[53]	**pCASL**[13]	**FAIR**[108]
Brain						
Voxel size (mm)	3x3x7	3x3x7	3x3x7	3x3x7	3x3x7	-
# slices	17	17	17	17	17	-
Recovery after presaturation (ms)	2000	2000	2000	2000	-	-
TR (ms)	4260	4260	4610	4160	4170	-
# repetitions	28	28	28	28	28	-
Total scan duration (min:s)	4:07	4:07	4:27	4:01	4:01	-
Post-labeling delay (ms)	1600	1600	[1150,820]	1500	1800	-
Background suppression (ms)	[50,1150]	[50,1150]	[20,620]	[560,580,1140]	[112,1350]	-
Cut-off velocity or acceleration	2cm/s	1.8m/s^2	2cm/s	2.8cm/s	-	-
Duration labeling module (ms)	50	50	50	48	1800	-
# labeling modules	1	1	2	1	1	-
VS-crushing during or before acquisition (cm/s)	2	-	2	3	-	-
Kidney [PB/FB]						
Voxel size (mm)	3x3x6	3x3x6	3x3x6	3x3x6	3x3x6	3x3x6
# slices	5	5	5	5	5	5
Recovery after presaturation (ms)	4908/3000	4908/3000	4130/3000	4908/3000	-	-
TR (ms)	6500/4600	6500/4600	6500/5380	6500/4630	6500/6340	6500/4750
# repetitions	21	21	21	21	21	21
Total scan duration (min)	4:46/3:22	4:46/3:22	4:46/3:56	4:46/3:23	4:46/4:39	4:46/3:29
Post-labeling delay	1200	1200	[1150,820]	1200	1500	1400
Background suppression (ms)	[100,940]/ [100,925]	[100,940]/ [100,925]	[20,660]/ [20,650]	[350,650,1080]/ [350,650,1070]	[1520,2530]/ [1520,2530]	[500,1020]/ [500,1020]
Cut-off velocity or acceleration	5cm/s	1.4m/s^2	5cm/s	5cm/s	-	-
Duration labeling module (ms)	50	50	50	48	1800	15
# labeling modules	1	1	2	1	1	1
VS-crushing during or before acquisition (cm/s)	5	-	5	5	-	-
Q2TIPS[109]: five 120mm saturation slabs evenly spaced	-	-	-	-	-	1200-1300ms

Table 1. Scan parameters used brain and kidney. For the bottom (kidney) panel; settings that differ between the paced and free-breathing scans are indicated as [paced-breathing]/[free-breathing]. For all scans hyperbolic secant pulses were used as background suppression pulses. Abbreviations: VSASL = velocity selective arterial spin labeling, AccASL = acceleration-selective ASL, mm-VSASL = multiple velocity selective arterial spin labeling, VSI-ASL = velocity selective inversion, pCASL = pseudo-continuous ASL and FAIR = flow alternating inversion recovery.

The flow-based ASL-techniques did not require additional planning of a labeling slab. For FAIR the selective labeling slab, and thus the imaging volume, was planned such that it excluded the aorta, to ensure labeling of the aorta. The pCASL labeling slab was planned perpendicular to the aorta. Care was taken to not place the pCASL labeling slab too inferiorly to minimize the chance of the kidneys moving into the labeling slab during breathing, and also not place it too superiorly to minimize negative effects on labeling efficiency from field-inhomogeneities at the air-tissue interface of the lungs.

In addition to the ASL-scans, an M_0 and a T_1-map was acquired with the same planning as the ASL-acquisition. The M_0-scan was acquired in paced breathing for calibration of the ASL-signal, using the same acquisition as the ASL-scans, with ASL-labeling turned off and using a TR of 6500ms. The T_1-map was acquired for segmentation of kidney cortex and medulla. It was acquired using a cycled multi-slice inversion-recovery sequence[110] with 11 inversion times ranging between 42ms and 2030ms, and a multi-slice single-shot EPI acquisition. Resulting in total scan duration of 1min18.

A B_1-map was acquired in two subjects, and in one of these subjects an additional VSI-ASL scan was acquired without BGS, using 10 repetitions. These additional scans were acquired to investigate the origin of an artefact of VSI-ASL in kidney that became apparent during scanning. The B_1-map was acquired using a dual-TR method[111] with a TR of 30ms and 150ms, and a gradient spoil factor of 20. The B_1-map received the same planning as the ASL-acquisition. See the Supporting Information S1, and Supporting Information Figure S1 and S2 for these results and further simulations on the VSI-ASL artefact.

Postprocessing

Using SPM12[112], the brain ASL-scans were first realigned and co-registered to the T_1w-scan, and later transformed to MNI space and smoothed (kernel width=8x8x8mm). Using Mevislab[113] (MeVis Medical Solutions AG, Fraunhofer MEVIS, Bremen, Germany), all kidney scans were co-registered to each other using a group-wise image registration method[114], separately for left and right kidney.

The ASL subtraction images (ΔM_i) were normalized by M_0 and averaged over all n repetitions to obtain a perfusion-weighted signal (PWS) map and enable inter-subject comparison.

$$\text{PWS}\ [\%] = \frac{1}{n}\sum_{i=1}^{n}\frac{\Delta M_i}{M_0}$$

Voxel-wise tSNR was calculated by dividing the average ASL-signal over time ($\mu_{\Delta M,voxel}$)by the standard deviation of the ASL-signal over time per voxel ($\sigma_{\Delta M,voxel}$).

$$\text{tSNR}_{voxel} = \frac{\mu_{\Delta M,voxel}}{\sigma_{\Delta M,voxel}}$$

Whole-brain masks were created by thresholding the M_0-image, and whole-kidney masks were created by manually drawing kidney contours on the M_0-image. These masks were used for visualization. For the tSNR-graphs, gray matter masks were generated based on the T_1w- brain scans using the SPM12 Toolbox[112]; voxels with >70% gray matter were included in the mask. Cortex-/medulla-/ and high intense fluid masks were generated based on the kidney T_1-map using an intensity histogram to manually threshold the image. This study showed artefacts in the VSI-ASL kidney images in some subjects with the severity of the artefact varying greatly between subjects. To enable a fair comparison between results, individual artefact masks were manually drawn on the VSI-ASL images and the voxels inside the artefact mask excluded for the tSNR analysis of VSI-ASL. Additional scans and simulations on the VSI-ASL artefact in kidney can be found in the Supporting Information S1, and Supporting Figure S1 and S2.

Statistical analysis

For both the brain and kidney dataset, a repeated-measures ANOVA in combination with a Tukey post hoc test was applied to test whether there are significant differences in terms of tSNR between the different ASL-techniques, using P=0.05. Data is reported as mean ± standard deviation (STD).

To study the effect of visual stimulation on brain PWS, a voxel-wise repeated-measures ANOVA was performed to test whether the PWS-values acquired during rest and during visual stimulation conditions significantly differed from each other. All PWS repetitions (without averaging) of all subjects were used as input, setting subjects as between-group factor. Analysis was performed after transforming the PWS-maps to MNI-space. A Bonferroni correction was applied to correct for multiple testing, resulting in P=2.6e-7.

The effect of breathing strategy was evaluated using tSNR per unit time, to compensate for the shorter TR of the free-breathing scans. The mean tSNR-values in cortex were divided by the square-root of the time it takes to acquire one label-control pair.

$$\text{tSNR}_{per\ unit\ time}\left[s^{-1/2}\right] = \frac{tSNR}{\sqrt{2 * TR}}$$

A paired Student's t-test was used to test whether the tSNR per unit time differed significantly between scans acquired in paced- and free-breathing, using P=0.05.

RESULTS

Brain

PWS- and tSNR-maps of a representative subject are shown in Figure 2. Comparison of PWS-maps between ASL-techniques showed that VSI-ASL had a similar spatial pattern as the reference sequence, i.e. pCASL. Mm-VSASL showed very high signal in CSF-rich areas. VSASL and AccASL also both showed higher signal in areas with CSF, although to a lesser degree than mm-VSASL.

Figure 3 shows the distribution over subjects of the mean tSNR in gray matter, for all ASL-techniques. VSASL, AccASL, mm-VSASL, VSI-ASL and pCASL all have similar mean tSNR in gray matter without significant difference ($p>0.05$), although the standard deviation of the tSNR over subjects is larger for VSASL and mm-VSASL (tSNR mean ± standard deviation VSASL: 1.07±0.52, AccASL: 1.27±0.24, mm-VSASL: 1.36±0.55, VSI-ASL: 1.18±0.12, pCASL: 1.10±0.09).

Next, the ability to measure small increases in perfusion upon visual stimulation was compared between all ASL-techniques. VSI-ASL and pCASL detected the visual cortex most robustly, as evidenced by the highest number of voxels in the visual cortex that showed statistically significant increased PWS (Figure 4). VSASL, AccASL and mm-VSASL showed less power: less voxels showed significant increases in perfusion and p-values were higher.

Kidney

One subject was excluded due to excessive through-plane motion during the scans, leaving five subjects available for analysis.

Figure 5a shows representative PWS-maps from one subject. The flow-based ASL-techniques all showed clear corticomedullary contrast with spatially homogeneous signal in the cortex region, similar to the two reference techniques, i.e. FAIR and pCASL. Between the flow-based techniques VSI-ASL and AccASL show a slightly higher PWS compared to the rest. In general though, flow-based techniques had a similar PWS-intensity as pCASL, but clearly lower than FAIR. The flow-based ASL-techniques displayed small abnormalities at locations that are part of the collecting system, indicated by the green arrows in Figure 5a. In addition, negative signal was sometimes observed in the medulla, especially for VSI-ASL.

A similar pattern was observed on group-level in the tSNR graphs of Figure 5b; all flow-based ASL-techniques showed a similar tSNR as pCASL, but significantly lower than FAIR in cortex (tSNR mean ± standard deviation VSASL: 1.59±0.21, AccASL: 1.54±0.41, mm-VSASL: 1.37±0.34, VSI-ASL: 1.62±0.36, pCASL: 1.79±0.56, FAIR: 4.61±0.71) ($p < 0.05$) as

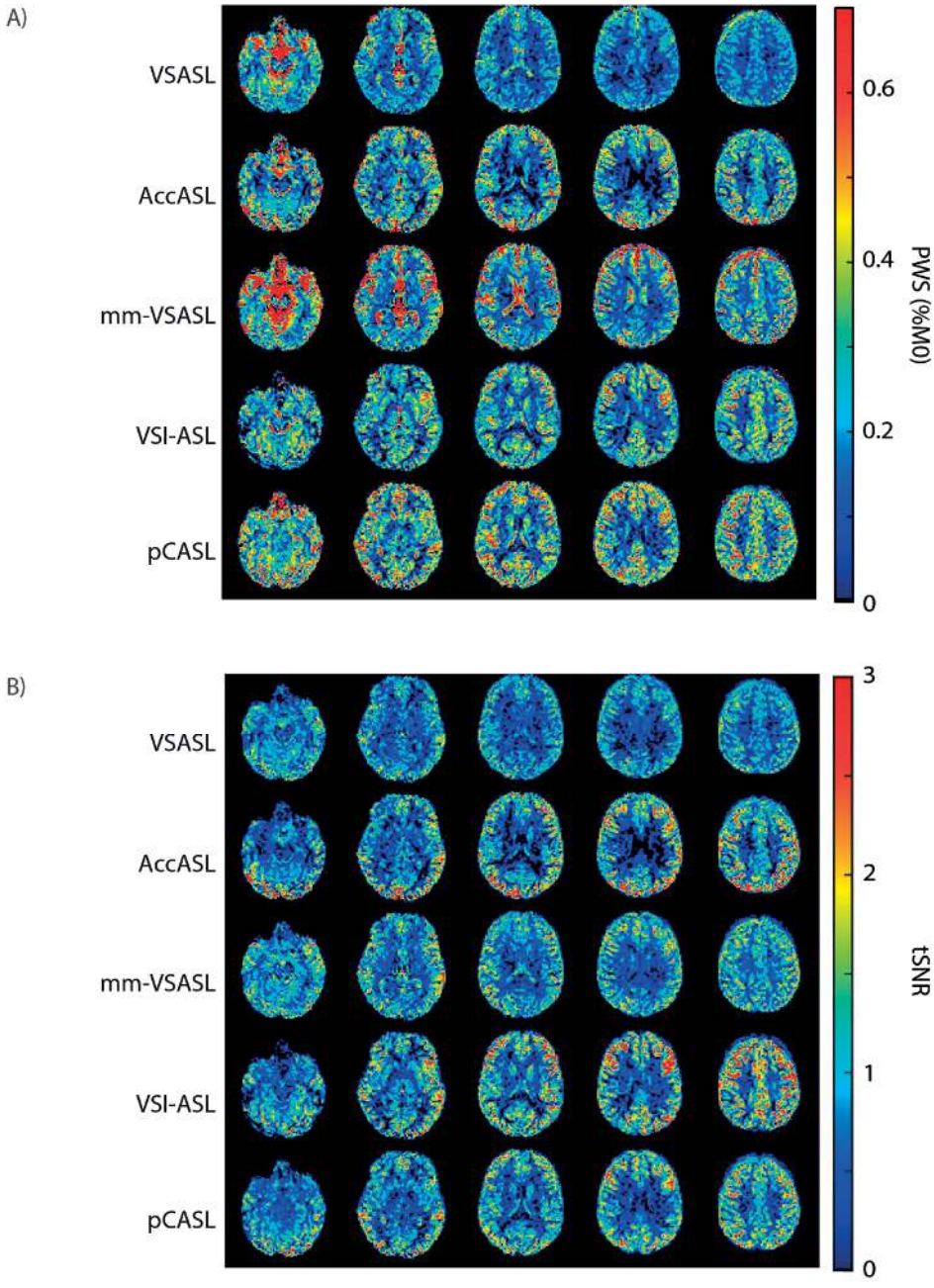

Figure 2. A) Brain perfusion-weighted signal (PWS-) maps of a representative subject. As expected, mm-VSASL and to a lesser extent VSASL and AccASL showed some T_2- and/or diffusion-weighting[43], [95], [96]*, illustrated by the high signal in areas rich in CSF B) Temporal signal-to-noise ratio (tSNR) maps of a representative subject.*

well as medulla (VSASL: 0.43±0.11, AccASL: 0.66±0.09, mm-VSASL: 0.50±0.06, VSI-ASL: 0.17±0.14, pCASL: 0.46±0.15, FAIR: 1.42±0.55) ($p < 0.05$). The tSNR in the medulla is notably lower than in the cortex. Note that in the tSNR-graphs in Figure 5b voxels that are part of the VSI-ASL artefact mask were not taken into account for the VSI-ASL images, see Supporting Information Figure S3 for the tSNR graphs including all voxels.

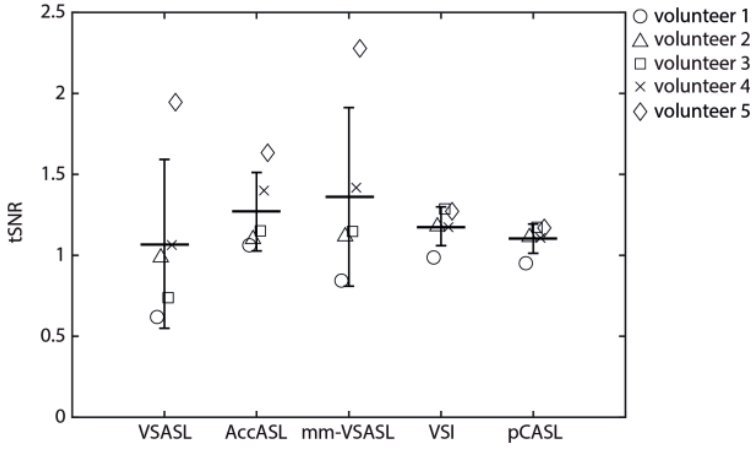

Figure 3. Distribution of mean temporal signal-to-noise ratio (tSNR) in gray matter over subjects, for all ASL-techniques. Middle bar represents the mean tSNR value over all subjects, and the vertical bars the standard deviation.

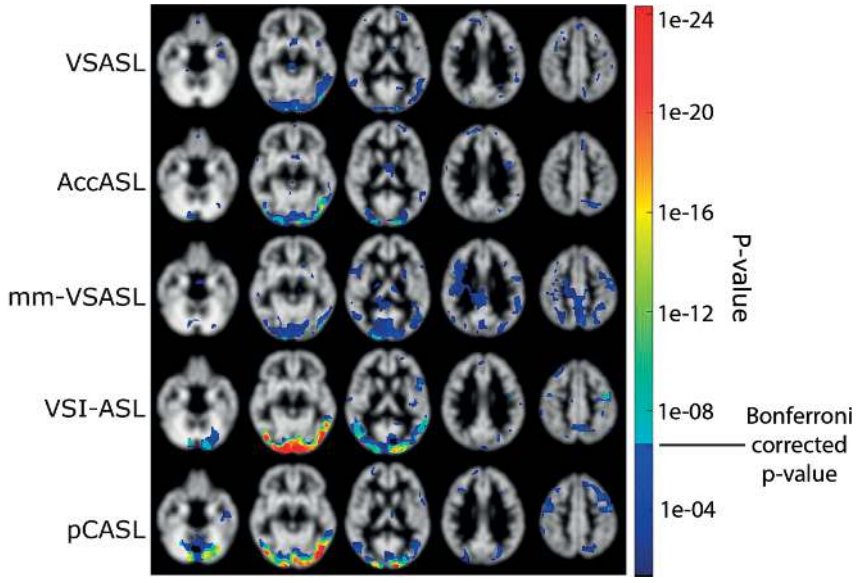

Figure 4. Visual activation maps of the brain averaged over all subjects, showing the voxels with a higher perfusion-weighted signal (PWS)-value during visual stimulus (watching cartoon) compared to rest (eyes closed). A Bonferroni correction was applied to correct for multiple testing, resulting in a significance level of P = 2.6e-7. Color indicates the P-value. Results are overlain on a gray matter segmentation. Five brain slices are shown.

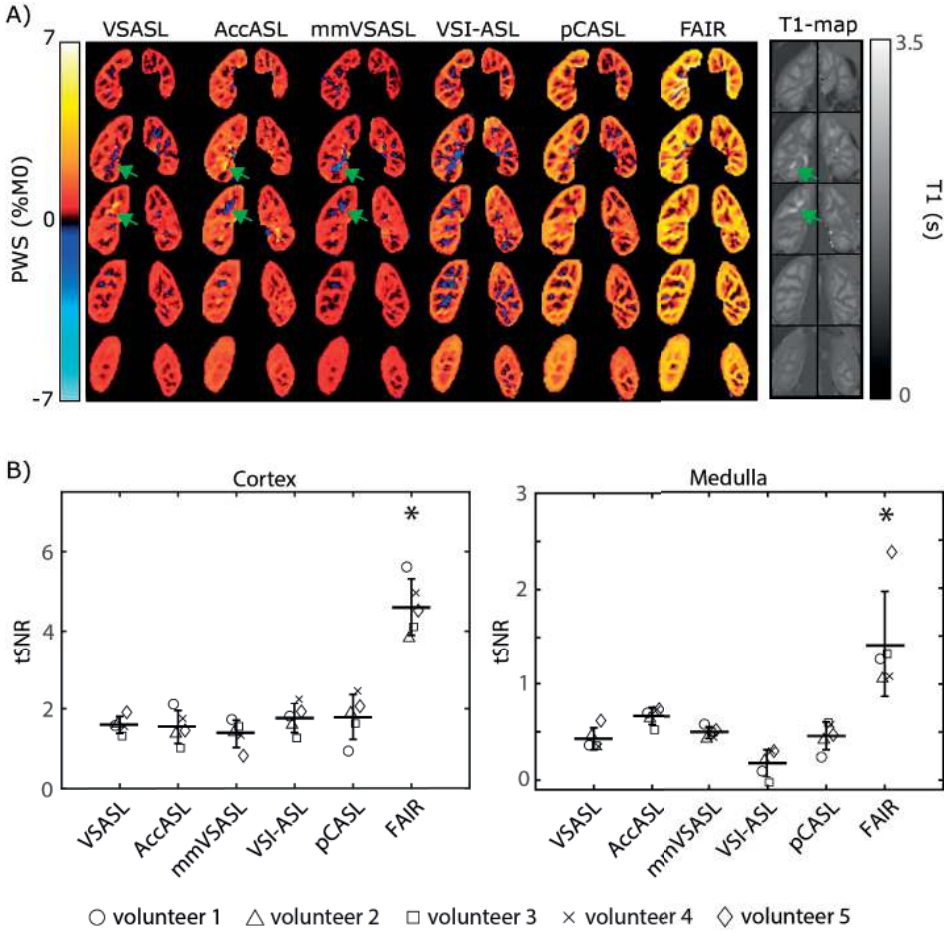

Figure 5. A) Kidney perfusion-weighted signal (PWS-) maps of a representative subject acquired during paced breathing. The green arrows indicate locations which are part of the collecting system, where the flow-based ASL-techniques displayed either intense positive or negative signal. B) Distributions of mean temporal signal-to-noise ratio (tSNR) in cortex and medulla over all subjects, for all ASL-techniques. FAIR had a statistically significant higher tSNR than all other ASL-techniques indicated by the asterisk ($p<0.05$), for both cortex and medulla. Note that for VSI-ASL the voxels that were part of the artefact mask were not taken into account.

Next, sensitivity of the flow-based ASL-scans to breathing strategy was investigated (Figure 6). VSASL, and AccASL both showed a reduction of ~14% in mean tSNR per unit time for the free-breathing condition, while hardly any reduction of tSNR per unit time was observed for mm-VSASL and VSI-ASL (resp. <0.01% and -0.03%). However, none of the flow-based ASL-techniques showed a statistically significant decrease in tSNR per unit time. Only FAIR, showed a statistically significant lower tSNR per unit time for the free-breathing condition ($P < 0.05$), although the difference was small ~14.2%, see Figure 6.

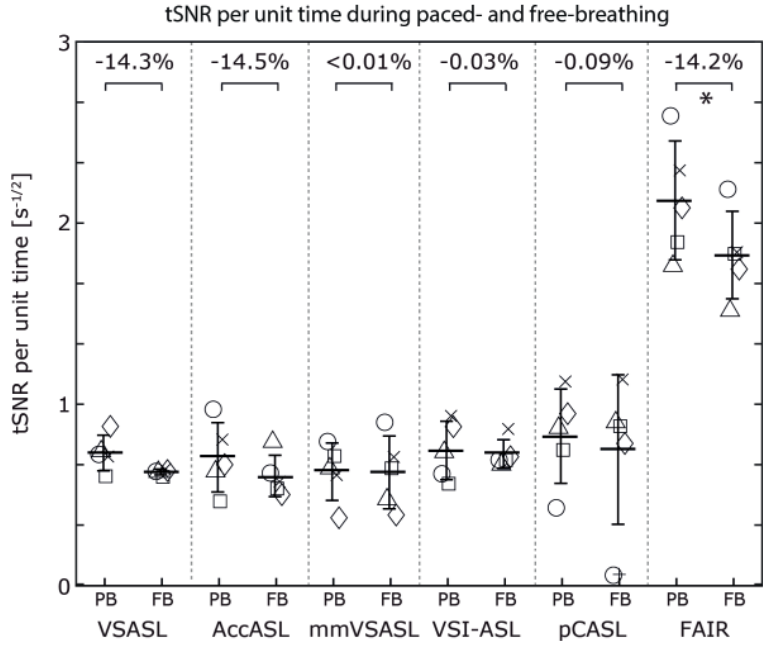

Figure 6. Temporal signal-to-noise ratio (tSNR) per unit time for all subjects in the kidney cortex, during paced- (PB) and free-breathing (FB). At the top the mean paired difference between paced and free-breathing tSNR per unit time is given in percentages. Only FAIR has a statistically significant lower tSNR per unit time during free-breathing, but this difference is small (-12.2%).

DISCUSSION

This study has shown that flow-based ASL-techniques are feasible in both the brain and kidneys at 3T, enabling planning-free ASL-measurements with intrinsically reduced sensitivity to transit-time artefacts. In brain, results showed that all flow-based ASL-techniques had comparable robustness of the signal (tSNR) to the reference pCASL. However, only VSI-ASL showed similar sensitivity as pCASL for picking up small increases in brain perfusion. In the kidneys, all flow-based ASL-techniques showed similar PWS and good corticomedullary contrast. However, compared to the reference technique FAIR, all flow-based ASL-techniques had significantly lower tSNR. The flow-based ASL-techniques proved to be robust to respiratory motion when using image registration, enabling free-breathing acquisition.

In brain, a comparable tSNR was found for all flow-based ASL-techniques (VSASL, AccASL, mm-VSASL, VSI-ASL) and pCASL. VSASL, mm-VSASL and AccASL showed a higher variability of tSNR over subjects than VSI and pCASL, although this could mainly be attributed to a single subject. Further inspection showed that this subject had a deviating CSF-system compared to the other subjects, as can be seen in Supporting Information Figure S4a. Possibly partial volume effects in combination with the inherent diffusion-weighting of VSASL, Ac-

cASL and mm-VSASL, can explain the increased tSNR in this subject compared to the others. See Supporting Information Figure S4b for a representation of the ASL-data in the gray matter segmentation.

In comparison, previously, a significantly lower tSNR for VSASL was found compared to AccASL and pCASL[51]. Discrepancy in the results could be due to the use of a lower flip angle of the adiabatic refocusing pulses in Ref. 17 compared to the current study. In the current study, adiabatic refocusing pulses were used with a higher flip angle and with a slower rotation of the effective B1-field that better satisfied the adiabatic condition. This resulted in a 50ms VSS-labeling module instead of 30ms. The gains from improved adiabaticity outweighed the losses from increased T_2-decay as a result of a longer duration.

Guo and Wong reported that ASL-signal of gray matter (treated as a direct indicator of spatial SNR) of mm-VSASL was significantly higher than VSASL, and was similar to that of pCASL[52]. In the current study tSNR was used to compare the different techniques instead of spatial SNR, to also take signal robustness into account. A similar tSNR for VSASL, mm-VSASL, and pCASL was found. When solely looking at the ASL-signal though, mm-VSASL did show a higher value than VSASL and pCASL, albeit with a larger standard deviation over time, see Supporting Information Figure S5. In addition, Guo and Wong used a BIR-8 implementation of VSASL[52], which has been shown to be more resistant to eddy currents and B_1-inhomogeneities[57], [115], instead of the VSASL-implementation shown in Figure 1a. Qin and van Zijl (2016) reported a similar tSNR between VSI-ASL and pCASL[53], and comparable values were measured in the current study.

Results in the brain showed that all flow-based ASL-techniques have similar tSNR to pCASL. However, tSNR provides information on ASL-signal stability over time, but does not provide evidence on the sensitivity of the technique to detect small changes in CBF. To test this, a mild visual stimulus was given. From the flow-based ASL-techniques, VSI-ASL showed a similar sensitivity to pick up changes in perfusion as pCASL, confirming a recent perfusion weighted functional MRI study[79], whereas VSASL, AccASL and mm-VSASL showed less power. The reason why VSASL, AccASL and mm-VSASL showed lower sensitivity to detect CBF-changes compared to VSI, even though they have similar tSNR, is probably due to the fact that they are more prone to subtraction errors due to e.g. diffusion. These errors contribute to a high tSNR, but do not contribute to the visual activation map. This, together with previous findings that VSI-ASL produces similar CBF-maps as pCASL[53], implies that VSI-ASL is the most promising flow-based ASL-technique for brain applications.

Diffusion-weighting of the VSASL-, AccASL- and especially mm-VSASL-signal, visible as high signal in CSF-related areas, has also been observed in previous studies[49], [51], [52]. Diffu-

sion sensitivity of VSASL, AccASL and mm-VSASL is caused by the fact that the VSS- and ASS-labeling module contains motion-sensitizing gradients and the control module does not. The mm-VSASL signal is especially affected, possibly because of the additional VSS-labeling module. A diffusion correction should be applied when using VSASL or mm-VSASL for quantification[97], to prevent overestimation of the CBF. AccASL cannot be quantified at the moment, since the bolus duration is unknown[51].

In kidneys, tSNR was comparable for all flow-based ASL-techniques and pCASL. However, compared to FAIR, all flow-based techniques had a significantly lower tSNR in both cortex as well as medulla. VSASL was previously compared to pCASL at 1.5T, and a lower whole kidney tSNR for VSASL compared to pCASL was reported[97]. The discrepancy in results is likely caused by a higher B_0-inhomogeneity at 3T reducing the labeling efficiency of pCASL, thereby reducing the benefits of pCASL with respect to VSASL.

The observed lower tSNR for flow-based ASL-techniques compared to FAIR could be caused by a lower labeling efficiency of the flow-based ASL-techniques: possibly because of a higher sensitivity to field-inhomogeneity or because of the dependence on flow-direction. Labeling by flow-based ASL is only sensitive to flow in a single direction, as determined by the orientation of the labeling gradients. Labeling-directions were chosen based upon the primary directions of flow, and also orthogonal to the direction of respiratory movement to mitigate possible bulk-motion artefact, as has been observed previously[97]. Besides this, previous studies in both brain[49] and kidney[97] have found little dependence of the VSASL-signal on the labeling-direction for a cut-off velocity of <4cm/s and 5cm/s in brain and kidney respectively. More research is necessary to be able to draw final conclusions the precise reason why FAIR performs better than flow-based ASL in the kidneys.

Although it was not the subject of the current study, the tSNR difference between the two standard techniques in kidney ASL: FAIR and pCASL, is noteworthy. We found a 3 times higher tSNR for FAIR compared to pCASL. Similar differences were found in a previous study[108], where a detailed discussion is provided on the reasons why pCASL performed worse than FAIR in kidney at 3Tesla, given that the opposite is true for the brain. Advantages of pCASL in brain include labeling closer to the imaging region and having a longer temporal bolus. However, these do not hold for kidneys. In the kidneys, the labeling plane of pCASL was planned 15cm above the kidneys and the temporal bolus of FAIR is increased since blood is labeled in most of the torso. This provides a possible explanation of the higher tSNR of FAIR that was found in this study. However, it is important to keep in mind that there are also downsides to using FAIR in kidneys. Coronal imaging is recommended for renal applications, so that through-slice motion due to respiration is minimized and blood is labeled closer to the kidney in the renal arteries. However, using coronal imaging comes with its own complications. First of

all, it is cumbersome to plan the selective labeling slab, since the aorta needs to be excluded. Secondly, coronal FAIR does not always allow full organ coverage, due to the constraint of excluding the aorta from the imaging region (between 54-80% of the kidney could be covered in the current study). This is why it is often used as a single-slice technique[62]. Flow-based ASL-techniques can provide a time-efficient alternative that guarantees whole organ coverage, albeit with lower tSNR.

In the current study a generally lower tSNR was found for kidney medulla compared to cortex, which was expected since the medulla has a lower perfusion than the cortex; only ~10% of renal blood flow reaches the medulla[18], [116]. However, the finding that FAIR has a significantly higher tSNR in medulla was not necessarily expected. Because of the longer transit times of medulla[108], one would expect that flow-based ASL-techniques are better suited to measure medullary perfusion than the spatially-selective ASL-techniques. However, it is likely that the cut-off velocity was still too high to label directly in the medulla. Unfortunately the cut-off velocity cannot be chosen lower than 5cm/s, without risking respiratory motion artefacts[97]. Nevertheless, results did show that the relative performance of flow-based ASL in the medulla was improved compared to that in the cortex.

Flow-based ASL in kidney also showed some artefacts in locations related to urine. This can be explained by the fact that while the ASL-module was played out, the collecting system will have high signal compared to kidney tissue, due to the short T_1 of urine. Small motion or diffusion-weighting of the urine signal will subsequently generate subtraction artefacts that can either be positive or negative.

Results showed that respiratory motion only plays a small role for flow-based ASL in kidney, when using image registration. A reduction in tSNR per unit time was observed during free-breathing for all flow-based ASL-techniques, although it was not statistically significant for any of the techniques. Indicating that up to a certain point, the shorter TR of free-breathing scans compensate for the reduction in tSNR by facilitating acquisition of more repetitions. This is in line with the paper by Robson et al (2009)[117], where they conclude that rejection due to motion-artifacts during free-breathing acquisition is offset by being able to acquire more data in the same scan time. In contrast to Robson et al, in the current study a FFE-EPI acquisition was used and no repetitions needed to be rejected because of motion.

In practice, the limited reduction in tSNR per unit time is outweighed by the great improvement to patient comfort and practicability. An additional benefit of acquiring scans in free-breathing is that images will be acquired during every respiratory state, which gives a more representative sampling of the hemodynamic state.

This study has shown that the performance of flow-based ASL-techniques in kidney is still less convincing than in brain. In kidney, all flow-based ASL-techniques had a significantly lower tSNR than FAIR, while in brain flow-based VSI-ASL provides comparable performance to pCASL.

Given the results in brain, VSI-ASL holds the most promise to improve the performance of flow-based ASL in kidney. However, VSI-ASL in kidney showed severe subtraction artefacts in some individuals. Additional scans and simulations were performed to investigate the underlying cause, see Supporting Information S1 and Supporting Information Figure S1 and S2. Results indicate that the combination of suboptimal inversion of the static tissue by VSI-ASL and of the BGS-pulses is likely the cause of the negative tissue signal that were observed in low-B_1 areas. The precise underlying cause and possible solution for the VSI-ASL artefacts observed in kidney warrants further research.

This study has some limitations. First of all, during the paced-breathing condition subjects were asked to shortly hold their breath during the image acquisition, but not necessarily during labeling. However, effects are expected to be small since a cut-off velocity (5cm/s) was chosen to prevent subtraction artefacts due to respiratory motion, and our results indeed did not show the typical high-intensity subtraction artefacts as described by Bones et al[97]. In addition, VSASL- and AccASL-labeling have been shown to depend on the cardiac cycle[118]. Effects are expected to average out when using a sufficient number of averages, but will still lower tSNR-values.

Secondly, as mentioned before, the current study employed a VSASL-implementation as described by Wong et al.[49] instead of the BIR-8 implementation of VSASL[57], [115], which has been shown to reduce eddy current effects as well as sensitivity to B_1. However, when using a PLD of 1500ms and a cut-off velocity of 2cm/s, similar CBF-maps were produced for both VSASL-implementations[57], so this is not expected to have had a major effect on our data.

Thirdly, balanced pCASL was used as one of the reference techniques. Recently, optimized unbalanced implementations of renal pCASL were presented in a limited number of subjects, to reduce sensitivity to B_0-inhomogeneities[103], [119]. Using one of the optimized implementations could improve the performance of pCASL as reported in this study. However, a separate shimming area at the labeling location is used in our pCASL implementation, which will reduce off-resonance artefacts when using balanced pCASL.

In addition, the PLDs used in renal mm-VSASL as taken from literature, were optimized for brain applications. Possibly the renal PWS of mm-VSASL could be improved by optimizing the PLDs specifically for kidneys.

Lastly, perfusion data in this study was not quantified. The main focus of the study was to provide a comparison on the performance of techniques without too much emphasis on differences in tracer kinetics and modelling assumptions that would result in technique-specific scaling factors. By dividing by M_0 inter-subject differences in scanner settings are accounted for and, without e.g. an additional subject-specific T_1 and labeling efficiency measurement, quantification would only add a technique-specific scaling factor. Quantitative comparison would especially be interesting when a gold standard reference, like PET, would be available.

In conclusion, this study has shown encouraging results for flow-based ASL in both brain and kidney. Flow-based ASL thus provides a promising planning-free and transit-time insensitive alternative for spatially-selective ASL in subjects with slow flow. VSI-ASL, as flow-based ASL-technique, shows the most promising results. In brain, VSI-ASL has a similar performance as the standardized pCASL, although in kidney more technical development at 3T, i.e. reduction of B_1-sensitivity, is necessary to match the performance of FAIR.

ACKNOWLEDGEMENTS

This work is part of the research program Drag and Drop ASL with project number 14951, which is (partly) financed by the Netherlands Organization for Scientific Research (NWO). We thank MeVis Medical Solutions AG (Bremen, Germany) for providing MeVisLab medical image processing and visualization environment, which was used for image analysis.

SUPPORTING INFORMATION

In a subset of the subjects severe ASL subtraction artefacts were observed in the VSI-ASL kidney images, mainly at the top of the kidneys. Additional scans were performed to investigate the origin of this artefact, which indicated that VSI-ASL, in its current form, is affected by severe B_1-sensitivity. Supporting Information Figure 1 shows example images of a subject with severely affected VSI-ASL images and a subject with minimally affected VSI-ASL images. Spatial overlap was seen for locations affected by the negative signal and locations of reduced B_1. In addition, a scan without BGS was performed in the same subject showing that no negative signal was present. However, the VSI-ASL signal remained spatially inhomogeneous over the cortical region, see Figure 7a.

Previous research has described the dependency of B_1 inhomogeneity with body geometry[60], [120]; larger body size with lower fat fraction is associated with a more severe B_1-inhomogeneity. This is also what we observed in this study; the VSI-images which were most affected by the inverted signal artefact were all tall lean subjects.

The spatial inhomogeneity of the VSI-ASL signal without background suppression suggests that the VSI-ASL implementation itself is affected. The current implementation of VSI-ASL is already more robust to B_0/B_1 compared to previous versions[53], [96], [121], [122], with regard to the velocity-selective profile. However, the inversion degree of the VSI-ASL pulse train is still sensitive to B_1, due to the use of hard pulses with low flip angles, applied at the beginning of each velocity-encoding step (Figure 1)[123], [124]. An interesting new work demonstrated better performance with VSI-ASL after optimizing the sequence for myocardial perfusion imaging[125]. A similar approach would also be interesting for renal, or other, applications.

However, results indicate that the observed artefacts are not only a result of B1-sensitivity of the VSI-labeling module, but also of the BGS-pulses. BGS is an essential element in renal perfusion ASL [36], [117], [126], but the combination of suboptimal inversion of the static tissue by VSI-ASL and suboptimal inversion of the BGS-pulses due to B1-sensitivity could cause the tissue signal to be negative.

To further understand this, a simulation was performed for the whole VSI-sequence using the timings described in the paper for kidney and the T_1 (1650ms) and T_2 (150ms) values of arterial blood. The simulation was performed for a B_1- and B_0-range appropriate for the kidneys, as measured in this study and supported by previous studies[127], [128]. See figure below for the subtracted ASL-signal. Please keep in mind that the signal between 'VSI with 3 BGS-pulses' and 'VSI with 2 BGS-pulses'/'VSI without BGS' is expected to be inverted, due to the use of

an uneven number of BGS-pulses, but the 'VSI with 2 BGS-pulses'/'VSI without BGS'-signal has been inverted to aid comparison. When looking at a B_1-values lower than 0.5 in the case of 'VSI with 3 BGS-pulses' the flowing spins have an inverted signal compared to the spins that have experienced a perfect B_1-field of 1.0. The same holds, but to a lesser degree, for 'VSI with 2 BGS-pulses'. In the case of 'VSI without BGS' this effect is not there. Furthermore the simulation shows that for non-perfect B_0 or B_1 variations in ASL-signal occur over velocity which may lead to variations in the ASL-signal.

The combination of imperfect inversion of the static tissue by the VSI-module in combination with imperfect inversion of the BGS-pulses could have caused the inverted ASL-signal present at the tip of the kidney found in several volunteers. This does not mean that the sequence should be run without BGS, but it does indicate that the BGS-pulses in its current shape and strength are not adequate for this application in the body.

Supporting Information Figures

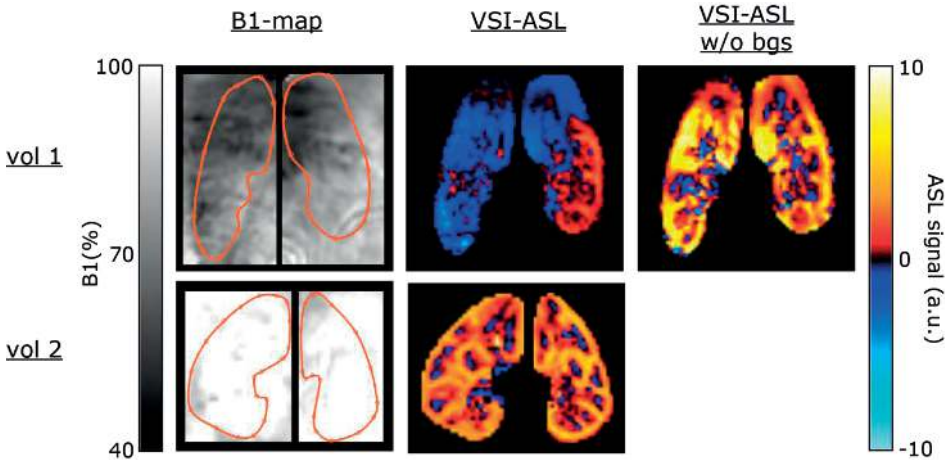

Supporting Information Figure S1. Data from a subject with severely affected VSI-ASL images (vol 1) and a subject with minimally affected VSI-ASL images (vol 2). A B1-map, including an overlay of the kidney contours, a VSI-ASL image with background suppression (BGS) and a VSI-ASL image without BGS are shown. Vol 1 shows clear negative signal in the VSI-ASL image. This artefact co-localizes with areas with reduced B1-power in the B1-map. Performing VSI-ASL without BGS showed less artefacts, although in that image there is still spatial variation of the VSI-ASL image. This indicates that the VSI-ASL artefacts are related to the B1-sensitivity of the BGS-pulses as well as the pulses in the VSI-ASL modules. These VSI-ASL images were acquired with 10 repetitions.

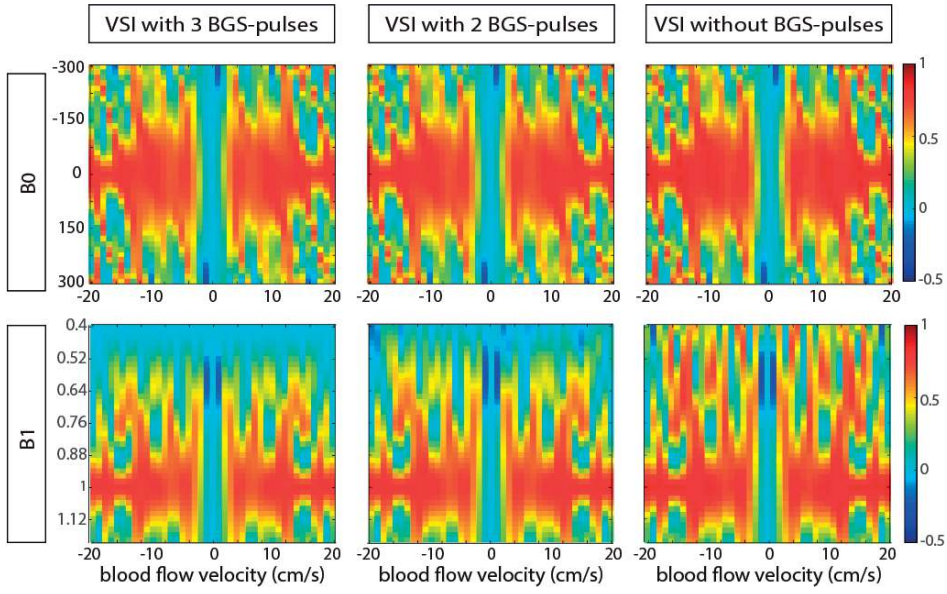

Supporting Information Figure S2. Simulation of the resulting ASL-signal for the whole VSI-sequence using three different background suppression (BGS) settings; with 3 BGS-pulses, with 2 BGS-pulses and without any BGS-pulses. Data was simulated using the settings for kidney, as described in the main paper. Simulation was done for a range of B0-values (top row) and a range of B1-values (bottom row). Results indicate that for VSI with 3 BGS-pulses and to a lesser degree VSI with 2 BGS-pulses negative signal can be expected for low B1-values (<0.5)

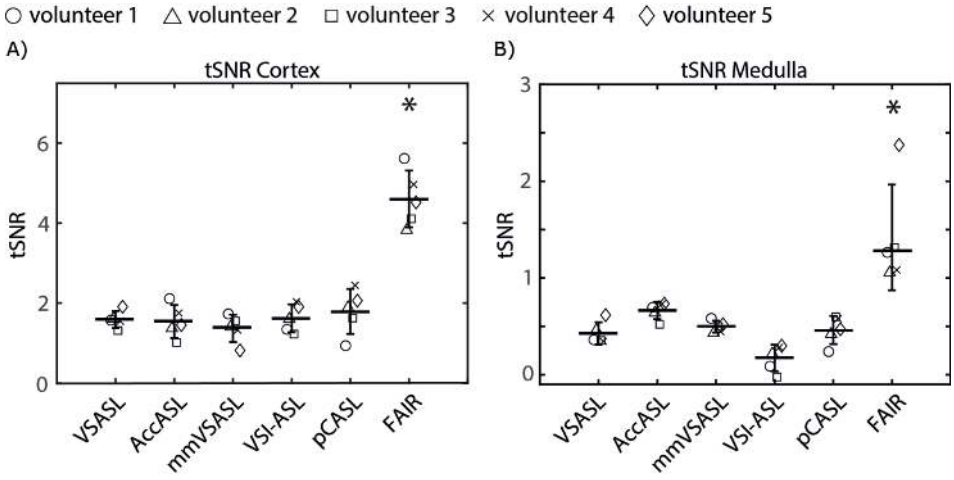

Supporting Information Figure S3. For all ASL-techniques the temporal signal-to-noise ratio (tSNR) in A) kidney cortex and B) kidney medulla using all voxels inside the mask, i.e. without excluding the artifact observed in VSI-ASL.

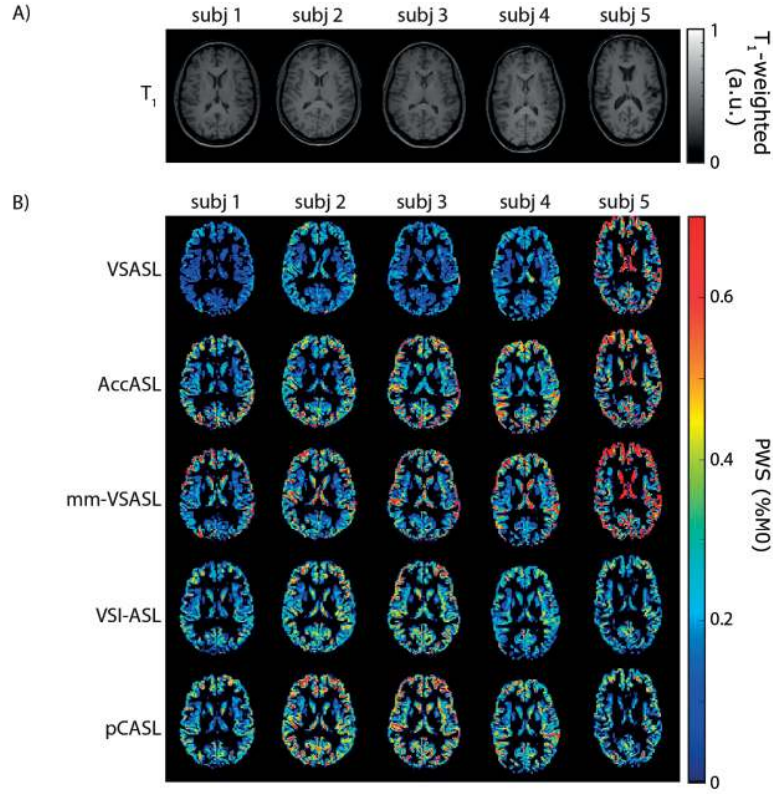

Supporting Information Figure S4. a) T1-weighted scan for all five subjects. Subject 5 appears to have a deviating CSF-system with larger ventricles than the other subjects. b) perfusion-weighted signal (PWS) in the gray matter mask. Columns represent the five subjects, and rows the five ASL-techniques. One slice in the middle of the brain is shown.

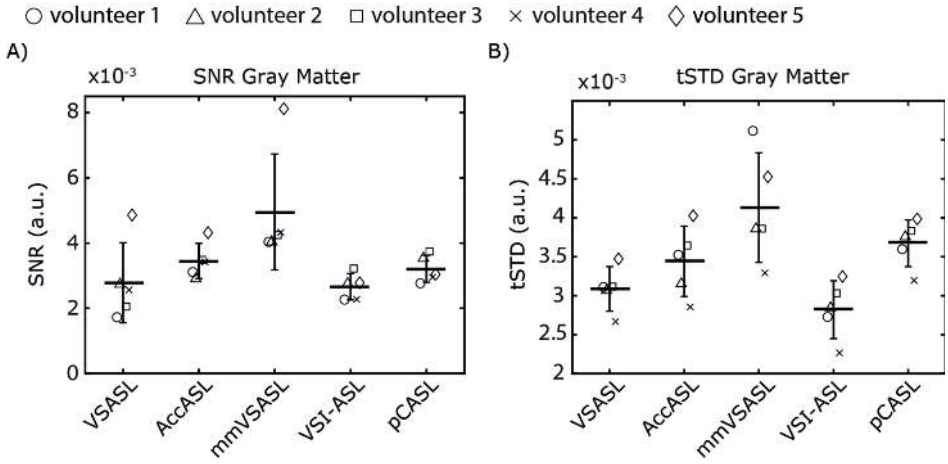

Supporting Information Figure S5. For all ASL-techniques the A) ASL-signal of gray matter, treated as direct indicator of spatial signal-to-noise ratio (SNR) and B) temporal standard deviation (tSTD) in the gray matter in brain.